

Research paper

The validity of generic trends on multiple scales in rock-physical and rock-mechanical properties of the Whitby Mudstone, United Kingdom

L.A.N.R. Douma^{a,*}, M.I.W. Primarini^a, M.E. Houben^b, A. Barnhoorn^a^a Faculty of Civil Engineering & Geosciences, Delft University of Technology, PO-box 5048, 2600GA Delft, The Netherlands^b Faculty of Geosciences, Utrecht University, PO-box 80.021, 3508TA Utrecht, The Netherlands

ARTICLE INFO

Article history:

Received 9 January 2017

Received in revised form

15 March 2017

Accepted 24 March 2017

Available online 28 March 2017

Keywords:

Posidonia shale

Young's modulus

Strength

Velocity anisotropy

Heterogeneity

Petrophysics

ABSTRACT

Finding generic trends in mechanical and physical rock properties will help to make predictions of the rock-mechanical behaviour of shales. Understanding the rock-mechanical behaviour of shales is important for the successful development of unconventional hydrocarbon reservoirs.

This paper presents the effect of heterogeneities in mineralogy and petrophysical properties on the validity of generic trends on multiple scales in rock-mechanical and rock-physical properties of the Whitby Mudstone. Rock-mechanical laboratory experiments have been performed on Whitby Mudstone samples from multiple outcrops within five kilometres laterally in order to investigate the heterogeneity and possible trends on an outcrop scale. Unconfined compression tests and acoustic measurements have been conducted to obtain the rock-mechanical properties, including rock strength, Young's modulus, Poisson's ratio, and velocity anisotropy. The rock-physical properties, including mineralogy, porosity, and matrix density, were measured using X-ray fluorescence and helium pycnometry. Various methodologies have been applied to the resultant data in order to derive different brittleness indices.

Significant heterogeneity in rock-mechanical and rock-physical properties is present on an outcrop scale. There is no obvious correlation between mineral content and rock-mechanical properties on an outcrop scale in the Whitby Mudstone. Comparison with shales from different basins show, however, correlations between composition and elastic properties. The presence of significant heterogeneities on an outcrop scale and between shales from different basins make it difficult to find generic trends in rock-physical and rock-mechanical properties.

© 2017 Elsevier Ltd. All rights reserved.

1. Introduction

The development of shale gas reservoirs generally requires hydraulic fracturing. Anisotropy, such as bedding planes, faults, and joints, strongly influences the fracture propagation and overall fracture geometry (Warpinski and Teufel, 1987). The presence of a bedding plane may provide a good fracture barrier (Warpinski and Teufel, 1987). Fracture initiation and propagation is also dependent on the rock-mechanical properties. These properties are required to understand the strength and stiffness of the shale, in order to determine whether the shale will be brittle enough to initiate fractures (Josh et al., 2012). For example, low Young's modulus and high Poisson's ratio shales are generally ductile, and allow fracture closure and self-healing (Britt and Schoeffler, 2009; Josh et al.,

2012). The anisotropy and rock mechanical properties are, in turn, controlled by shale fabric, mineralogy, and organic content (Dewhurst and Siggins, 2006; Vernik and Liu, 1997). However, shale gas reservoirs are heterogeneous formations whose mineralogy, organic content, maturity, and microstructure vary significantly on various scales (Dewhurst and Siggins, 2006; Houben et al., 2016a, b; Passey et al., 2010; Vernik and Liu, 1997). This heterogeneity complicates predictions of fracture behaviour and can lead to erroneous interpretations when upscaled to wireline-log, outcrop, or reservoir scale. Hence, understanding the controls on mechanical behaviour and anisotropy is important for the successful development of hydrocarbon reservoirs (Ewy et al., 2010).

Previous studies have shown that the anisotropy in shale gas reservoirs is caused by the alignment of platy clay minerals and organic material, fractures, stresses, and the level of maturity (Fjær and Nes, 2014; Sondergeld and Rai, 2011; Sone and Zoback, 2013; Vernik and Liu, 1997). The rock-mechanical properties depend on mineralogical and petrophysical properties, including clay and

* Corresponding author.

E-mail address: l.a.n.r.douma@tudelft.nl (L.A.N.R. Douma).

organic content, shale fabric, porosity, water content, and anisotropy (Fjær and Nes, 2014; Rybacki et al., 2016; Sone and Zoback, 2013). Sone and Zoback (2013) showed a correlation between clay and organic matter content, and elastic properties. Such correlations in rock physics help to predict the rock-mechanical behaviour of shales, improving predictions of the fracture response in shales. However, these correlations, are obtained by comparing a wide range of relatively quartz-rich shales from different basins, including other Posidonia shales, Barnett, Haynesville, Fort St. John, and Eagle Ford shale (e.g., Britt and Schoeffler, 2009; Sone and Zoback, 2013; Vernik and Liu, 1997). Little effort has been made on the applicability of these trends in clay-rich shales originating from a single basin on an outcrop scale.

This study examines the applicability of existing trends in rock-physical and rock-mechanical properties obtained from a wide range of quartz-rich shales on clay-rich shales from a single basin. Petrophysical and rock-mechanical analyses of relatively quartz-rich US shales is extended to the petrophysics and geomechanics of relatively clay-rich shales, since these clay-rich shales are a potential target for future shale gas exploration in Northwest Europe. Considerable amounts of gas are potentially present in these clay-rich shales, but the degree of brittle deformation is a challenge that may hinder economic hydrocarbon production (Ter Heege et al., 2015; Van Bergen et al., 2013). Clay-rich shale samples were taken along a stratigraphic section in a single basin in order to investigate the heterogeneities and possible trends in rock-physical and rock-mechanical properties on an outcrop scale. Comparisons were made with a wide range of US shales from different basins to assess the validity of generic trends.

2. Materials and methodology

2.1. Sample material

The Early Jurassic Posidonia Shale Formation (PSF) extends from the Yorkshire Basin (locally named Whitby Mudstone Formation (WMF), across the Lower Saxony Basin and the Southwest German Basin (locally named Posidonia Shale Formation) into the Paris Basin (locally named Schistes Carton) (Hesselbo et al., 2000; Houben et al., 2016a; Littke et al., 1991) (Fig. 1). The PSF is an organic-rich black shale with a thickness of circa 10–70 m, averaging 30 m over the entire basin (Houben et al., 2016a; Zijp et al., 2015). It is a proven source rock for conventional reservoirs and is considered as a potential source rock for unconventional reservoirs in Northwest Europe (Herber and Jager, 2010; Houben et al., 2016a; Zijp et al., 2015). However, current available data of the PSF is limited (Zijp et al., 2015). The PSF is not exposed in the Netherlands and intact samples from cored well intervals of the Dutch PSF are lacking. Therefore, this study focuses on the time and depositionally-equivalent WMF as an analogue for the Dutch PSF (e.g., Houben et al., 2016b; Jenkyns, 1985).

The WMF can be subdivided in the Grey Shale Member, Mulgrave Shale Member, and Alum Shale Member (Powell, 2010). The Grey Shale Member consists of silty mudstone beds of calcareous siderite concretions (Grey Shale Bed) (Powell, 2010) (Fig. 1). The Mulgrave Shale Member comprises the Jet Rock Bed and Bituminous Shales Bed. The Jet Rock Bed is an oil-prone source rock and consist of bituminous dark grey mudstone with abundant ammonites (Powell, 2010; Zijp et al., 2015). The Alum Shale Member is less fossiliferous and contains grey silty mudstone, with calcareous bands and siderite concretions (Powell, 2010).

Samples were collected along the coastal cliffs north of Whitby, near Runswick Bay and Port Mulgrave (see also Houben et al., 2016a; Zhubayev et al., 2016). Twenty one mudstone samples were collected from the outcrops. Working on an outcrop enables

study of heterogeneities on multiple scales. In order to study the heterogeneity of the shales, samples were collected at different heights along 8 m of stratigraphic section, including the Grey Shale and Jet Rock Member, and within 5 km laterally. Shale blocks of about 30 by 30 by 6 cm were collected using a geological hammer and chisel (see also Houben et al., 2016a). The majority of the samples were taken from the Jet Rock Member because of its accessibility and high organic content (4–15%) (Hesselbo et al., 2000; Powell, 2010).

2.2. Sample preparation

Each shale block was cut in the field and packed in cling wrap to prevent it from drying. Twenty two cubic subsamples were cut out of larger blocks using a sawing machine cooled with air. Each sample was cut at a 90° angle with respect to the bedding plane (see also Zhubayev et al., 2016). The subsamples were manually sanded into cylindrical shapes and ground flat at both ends with a 30 mm diameter and 60 mm length. The cylindrical samples were not sealed and the water content was not controlled during sample storage and sample preparation. All prepared shale samples were analysed to investigate the mineralogical, petrophysical, rock mechanical, and anisotropy characteristics.

2.3. X-ray fluorescence

Geochemical analyses were performed on twelve shale samples using X-ray fluorescence (XRF) in order to determine the mineral composition and associated weight throughout the section. The analysed shale samples were powdered and dried in the oven at a temperature of 70 °C for at least 24 h. A spectrometer (Panalytical Axios Max WD-XRF) was used for XRF analysis measurements. Data evaluation was performed using the *Super Q5.0i/Omnian* software.

2.4. Helium pycnometry

Porosity and matrix density were measured on cores using the *Ultrapycnometer 1000 version 2.12* pycnometer. Helium (He) gas was used to measure the porosity and matrix density because of its small atomic dimensions enabling measuring pores with diameters down to nm-scale. The porosity values represent the effective porosity, connected to the samples outside, that was connected with pore throats wide enough for He to enter.

2.5. Rock-mechanical analyses

Ultrasonic P-wave (V_p) and S-wave (V_s) velocities of seventeen samples were recorded parallel (V_{90}) and perpendicular (V_0) to the bedding plane axis to derive the dynamic elastic properties and anisotropy. P-wave or S-wave transducer and receiver were coupled for the ultrasonic experiments. No axial or radial stress was applied. The central frequency of the transducer is 1 MHz. The dynamic elastic moduli are derived from the P-wave velocity (V_p), S-wave velocity (V_s), and density (ρ_m). The dynamic elastic parameters, including Young's modulus and Poisson's ratio, are derived from the elastic wave equation in isotropic media (e.g., Mavko et al., 2003). The dynamic Young's modulus is calculated from the following equation:

$$E_{dyn} = \frac{9K\mu}{3K + \mu} \quad (1)$$

where the bulk modulus (K) is expressed by $K = \left(V_p^2 - \frac{4}{3}V_s^2 \right) \rho_m$ and the shear modulus (μ) by $\mu = V_s^2 \rho_m$. The dynamic Poisson's

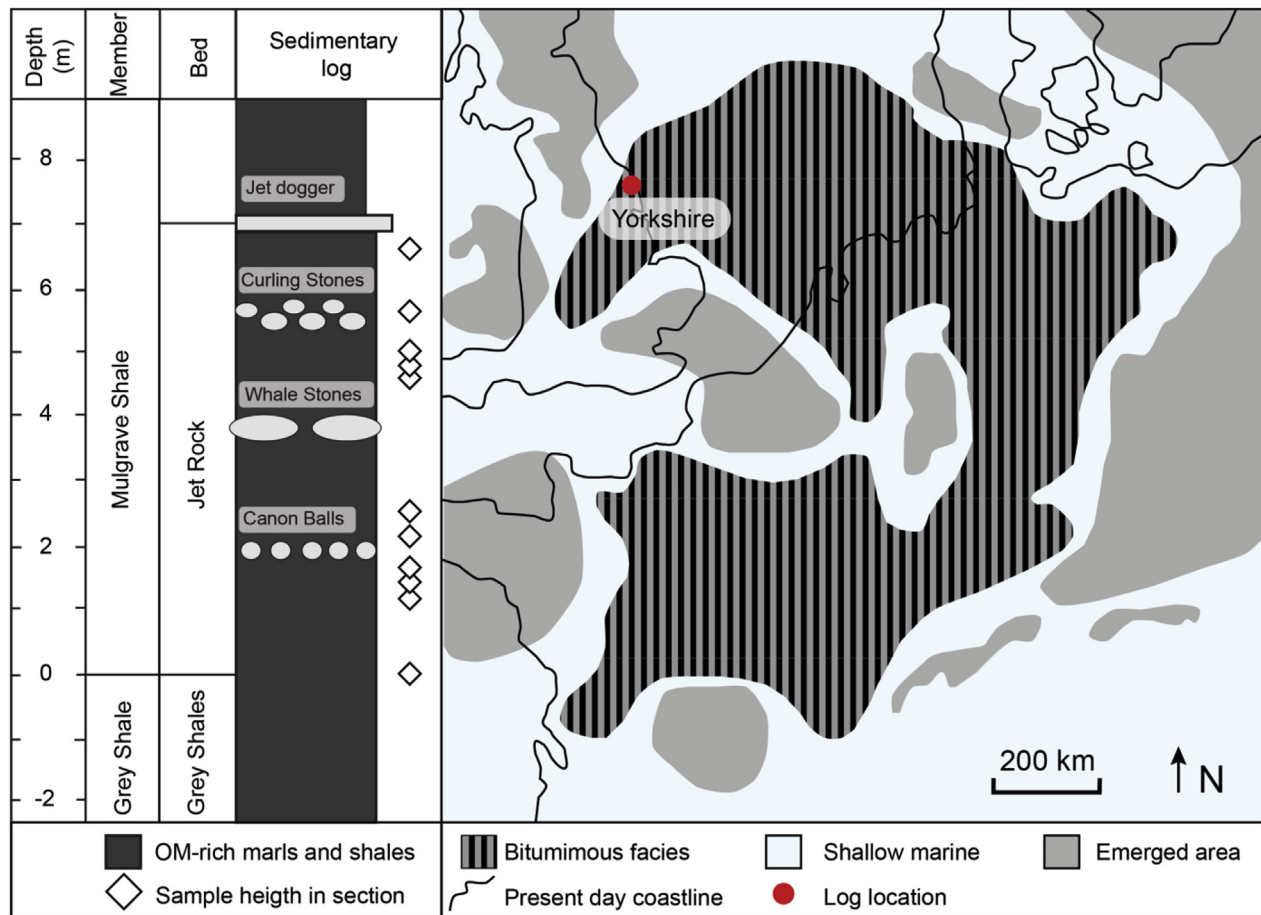


Fig. 1. Left: stratigraphic log of the Whitby Mudstone Formation (modified after Hesselbo et al., 2000; Houben et al., 2016a; Zijp et al., 2015) and sample height in the section. Right: simplified distribution of the Early Jurassic Posidonia Shale Formation (modified after Frimmel et al., 2004).

ratio is expressed by the elastic moduli K and μ following:

$$\nu_{dyn} = \frac{3K - 2\mu}{2(3K + \mu)} \quad (2)$$

Thomsen's parameters (ϵ , γ) (Thomsen, 1986) were used to describe the elastic anisotropy of the WMF (see also Zhubayev et al., 2016).

Unconfined compression tests were performed under room humidity conditions on fifteen dry shale samples to obtain the static elastic parameters (Young's modulus and Poisson's ratio) and rock strength. All experiments were conducted at room temperature (20 °C). Cylindrical samples were placed in a pressure bench with a 50–500 kN load frame and deformed until failure. The uniaxial compressive loading axis was oriented 90° to the bedding plane. The axial and circumferential strain were recorded by linear variable differential transformers (LVDTs) and extensometers mounted on the shale sample. Axial strain rates of 10^{-6} s^{-1} were used. The pore pressure was not controlled, as the injection of fluid in extremely low-permeable rocks is not feasible in a controlled manner and may introduce poroelastic effects (Sone and Zoback, 2013).

2.6. Brittleness indices

Brittleness is used to describe the brittle deformation behaviour of materials (Holt et al., 2015; Rybacki et al., 2015), where the

brittleness index is used to quantify the degree of brittle deformation behaviour of rocks. A high brittleness index (max. value of 1) indicates the highest degree of brittle deformation, whereas a low value (close to 0) indicates more ductile behaviour. However, there is not one definition of brittleness index (Holt et al., 2015, 2011; Hucka and Das, 1974; Rybacki et al., 2015; Yang et al., 2013). Four different definitions that could quantify the brittleness of the WMF were used (Table 1). A brittleness index based on mineralogy (B_1) (Jarvie et al., 2007), one based on the relation between elastic strain and total strain at failure (B_2) (Coates and Parsons, 1966), and two based on the combination of dynamic Young's modulus and Poisson's ratio (B_3 ; B_4) (Jin et al., 2014; Rickman et al., 2008).

3. Heterogeneities in the WMF

3.1. Mineralogy and petrophysics of the WMF

Basic mineralogical composition and petrophysical properties information such as total organic carbon (TOC), effective porosity for helium, and matrix density of the stratigraphic section are summarised in Fig. 2. The mineral composition of seven samples analysed by Houben et al. (2016a) were included in the section (Fig. 2a).

The main fraction of the mineralogy consists of clay minerals, mainly kaolinite and illite. The clay content varies throughout the Jet Rock Member from about 40 wt% to approximately 75 wt%. The

Table 1

Brittleness parameters as found in the literature to quantify the brittleness of the WMF.

Brittleness indices	Comments	References
$B_1 = \frac{Qtz}{(Qtz+C+Cl)}$	Qtz, C and Cl are weight fractions of quartz, carbonate, and clay, respectively.	Jarvie et al. (2007)
$B_2 = \frac{\epsilon_{el}}{\epsilon_{tot}}$	ϵ_{el} and ϵ_{tot} are the elastic strain and total strain prior to failure, respectively.	Coates and Parsons, (1966)
$B_3 = \frac{1}{2} \times \left(\frac{E_{dyn}(0.8-\phi)}{8-1} + \frac{\nu_{dyn}-0.4}{0.14-0.4} \right) \times 100$	E_{dyn} , ν_{dyn} and ϕ are dynamic Young's modulus [Mpsi], Poisson's ratio and porosity, respectively	Rickman et al. (2008)
$B_4 = \left(\frac{(E_{min}-E_{max}) + (\nu_{min}-\nu_{max})}{E_{max}-E_{min} + \nu_{max}-\nu_{min}} \right)$	E_{min} , E_{max} and ν_{min} , ν_{max} are the minimum and maximum Young's modulus and Poisson's ratio, respectively. E and ν are the Young's modulus and Poisson's ratio over depth.	Jin et al. (2014); Rickman et al. (2008)

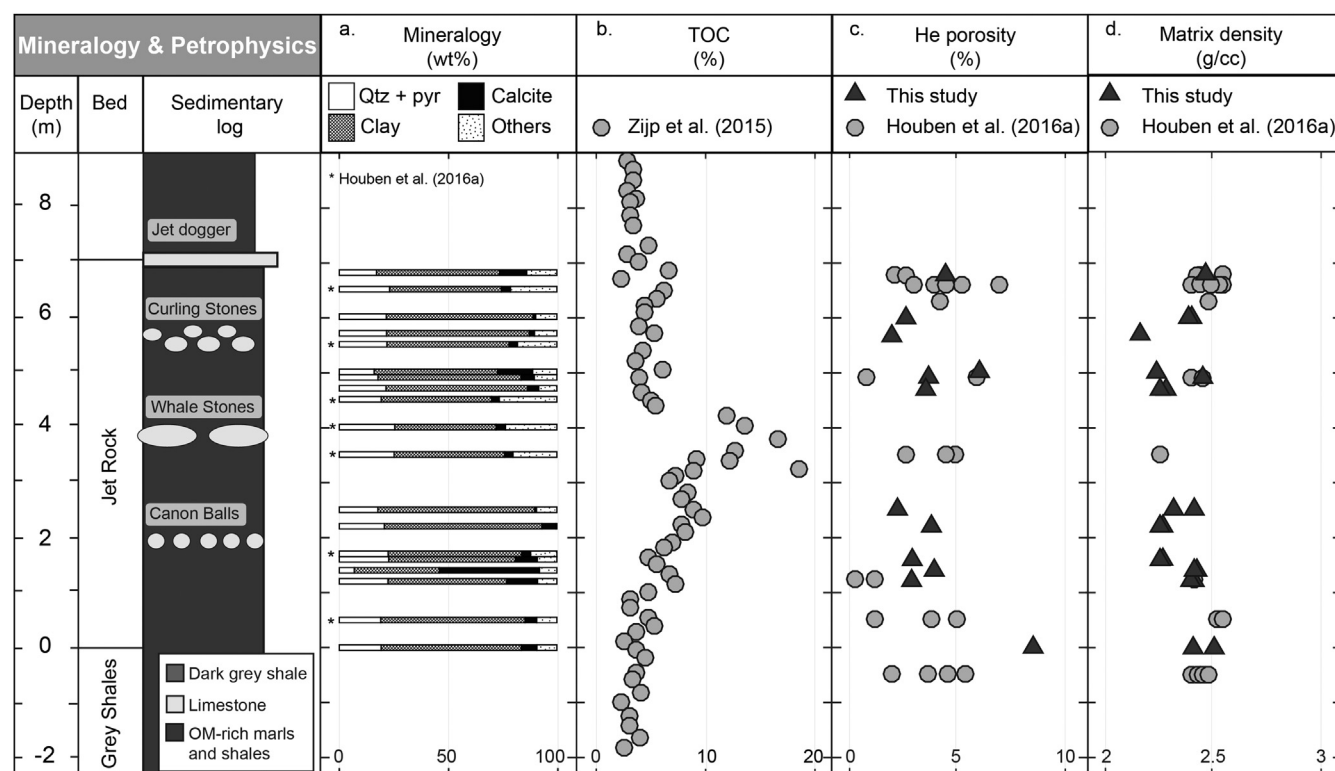


Fig. 2. Mineralogical composition and petrophysical properties of the Whitby Mudstone throughout the stratigraphic section. a. Mineralogical data from this study and Houben et al. (2016a). b. TOC data (Zijp et al., 2015). c. Connected porosity data from this study and Houben et al. (2016a). d. Matrix density from this study and Houben et al. (2016a).

clay content is higher at the base of the Jet Rock member than in its upper part. Additionally, the measured clay content seems to decrease in the vicinity of the Whale Stones. The combined quartz and pyrite content ranges from 18 to 29 wt%, with the maximum values occurring in the same interval as the Whale Stones. Locally, the section is calcite rich (up to 45 wt%), due to the presence of fossils.

Zijp et al. (2015) measured TOC throughout the section (Fig. 2b). The TOC measurements show a gradual increase from about 4% at the base of the Grey Shale Member to approximately 15% in the middle of the Jet Rock Member. Above this maximum, the TOC values decrease again to approximately 4% in the upper part of the Jet Rock Member. The level of maximum TOC values seems to correspond to maximum levels of quartz and pyrite content.

He porosity values from twenty-six samples of Houben et al. (2016a) are included in the section (Fig. 2c). The porosity values range from approximately 0.3% to approximately 5.2% (Fig. 2c). The porosity values vary between different samples taken from the same sample block as well as between different samples, implying that there is variation in porosity laterally on centimetre scale as well as vertically through the section (Houben et al., 2016a).

The matrix-density profile displays a vertical and lateral variation with maximum value of approximately 2.2–2.8 g cc⁻¹ (Fig. 2d). Measured matrix-density values are similar in the upper part and the base of the Jet Rock Member and decrease towards the middle of the Jet Rock Member.

3.2. Velocity and anisotropy of the WMF

P-wave velocities measured perpendicular to the bedding (V_{p0}) range between 1530 ms⁻¹ and 2520 ms⁻¹. P-wave velocities measured parallel to the bedding (V_{p90}) are higher, varying between about 2480 ms⁻¹ to about 3790 ms⁻¹ (Fig. 3a). S-wave velocities measured perpendicular to the bedding (V_{s0}) decrease from 1580 ms⁻¹ at the base of the Jet Rock Member to 1450 ms⁻¹ in the vicinity of the Whale Stones (Fig. 3b). The V_{s0} values increase again towards the top of the Jet Rock Member to a maximum of approximately 1760 ms⁻¹. The variation in recorded V_{s90} values is limited at the base of the Jet Rock Member, whereas they vary both laterally and vertically in the upper half of the Jet Rock Unit.

The Thomsen's notation is used to describe the elastic anisotropy of the shales. The P-wave anisotropy (ϵ) ranges from

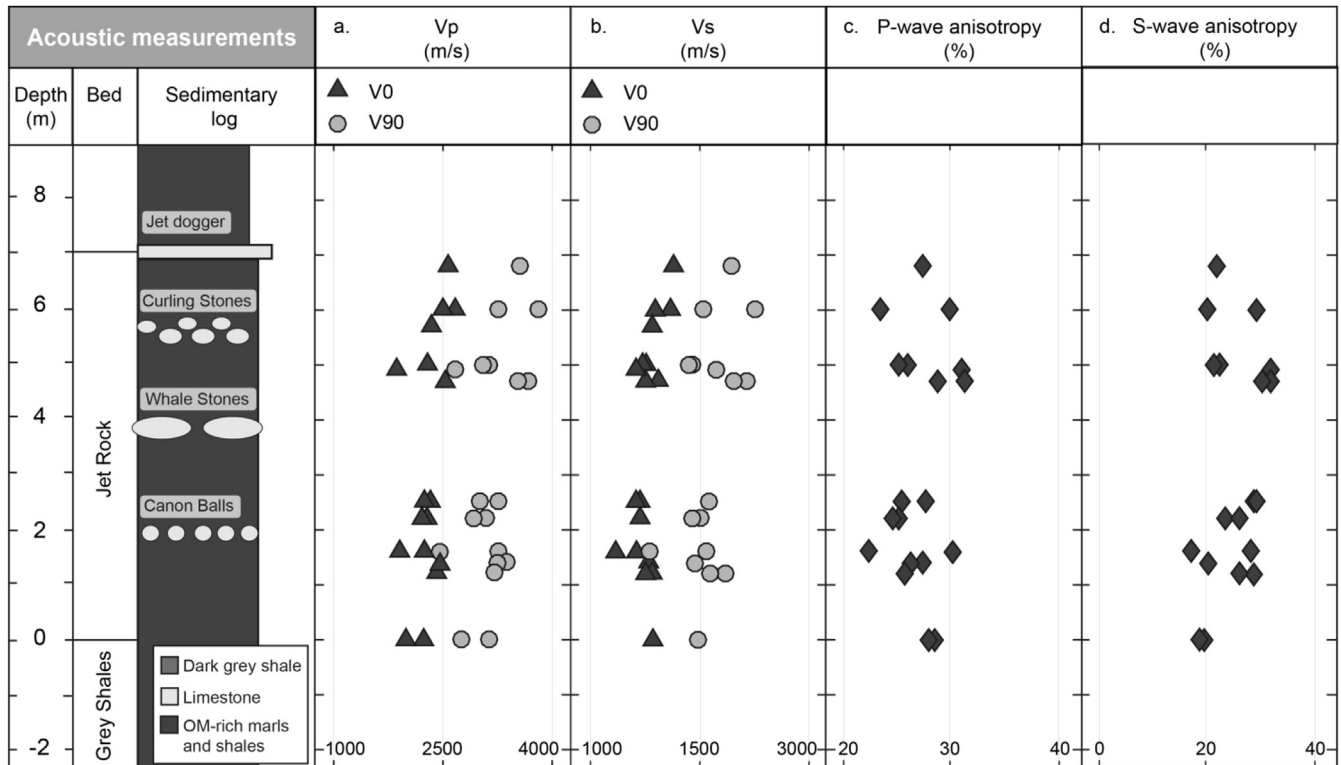


Fig. 3. Acoustic measurements of the Whitby Mudstone throughout the stratigraphic section. a. P-wave velocities parallel (V_{90}) and perpendicular (V_0) to the bedding. b. S-wave velocities parallel (V_{90}) and perpendicular (V_0) to the bedding. c. P-wave anisotropy (ϵ). d. S-wave anisotropy (γ).

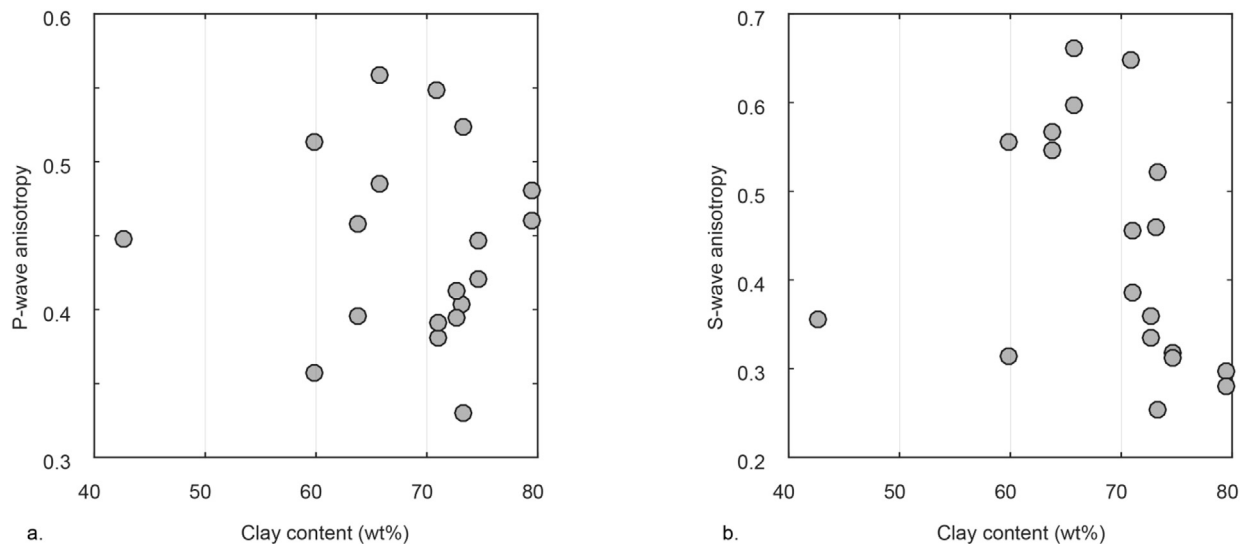


Fig. 4. Correlation between clay content and P-wave and S-wave anisotropy for the Whitby Mudstone samples. a. Clay content versus P-wave anisotropy (ϵ). b. Clay content versus S-wave anisotropy (γ).

approximately 33% to approximately 56% (Fig. 3c). The S-wave anisotropy (γ) varies from approximately 25% to approximately 66% (Fig. 3d).

The elastic anisotropy parameters are plotted against the amount of clay content for each Whitby shale sample (Fig. 4). Clay content is expected to have a great influence on the overall rock properties, since clay content is an important constituent of a shale (Sone and Zoback, 2013). The data shows that there is no clear correlation between the clay content and the P-wave and S-wave

anisotropy.

3.3. Rock mechanics of the WMF

The measured dynamic Young's modulus has a minimum value of 8 GPa at the base of the Jet Rock Member and increases to approximately 16 GPa towards the top of the Jet Rock Member (Fig. 5a). The dynamic Young's modulus is typically lower than the static Young's modulus. The static Young's modulus varies from

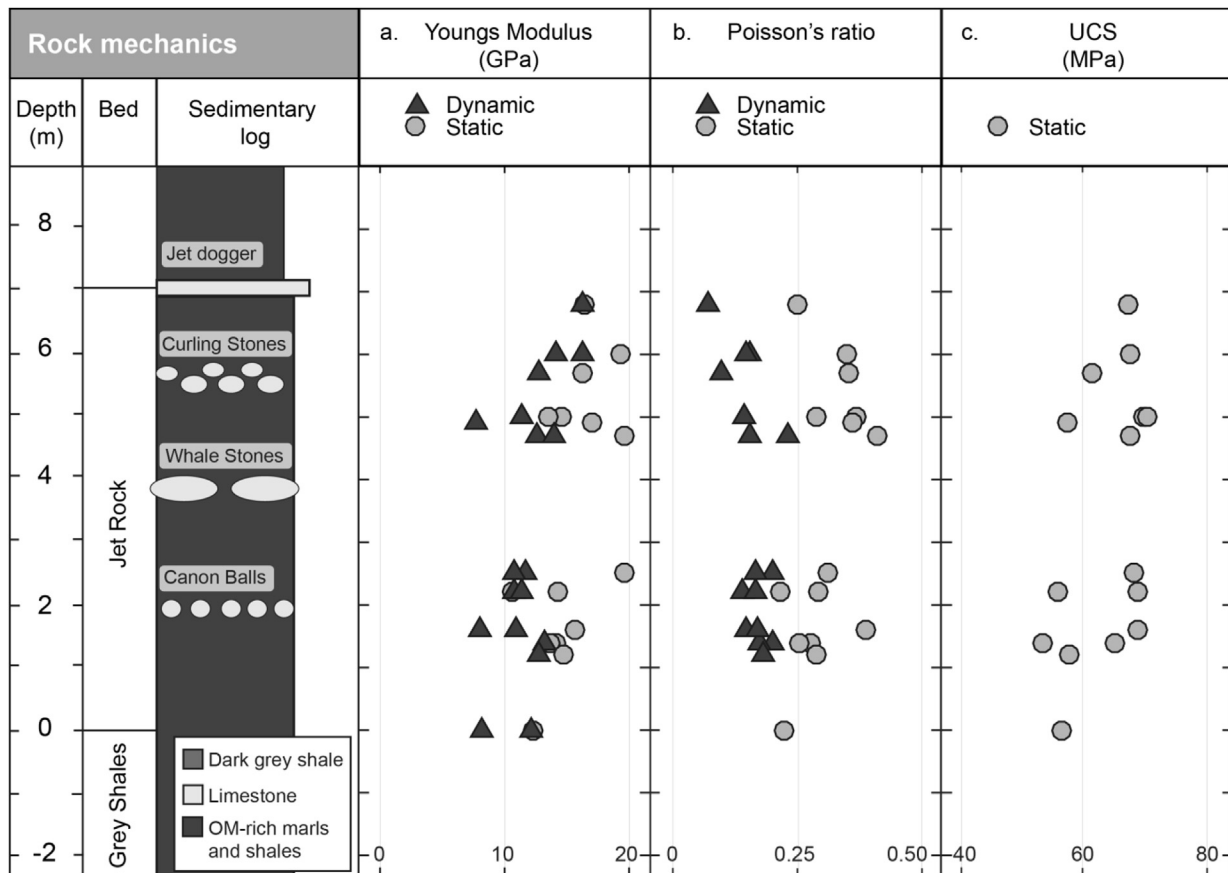


Fig. 5. Dynamic and static rock-mechanical properties of the Whitby Mudstone samples throughout the stratigraphic section. a. Dynamic and static Young's modulus versus section height. b. Dynamic and static Poisson's ratio versus section height. c. Uniaxial compressive strength versus section height.

approximately 12 GPa at the base of the Jet rock to approximately 29 GPa in the middle of the Jet Rock Member (Fig. 5a).

The dynamic Poisson's ratio shows a gradual decrease from approximately 0.22 at the base of the Jet Rock Member to approximately 0.15 at the top of the Jet Rock Member (Fig. 5b). There is limited variation in values of the dynamic Poisson's ratio in the lower half of the Jet Rock Member. The dynamic Poisson's ratio is lower compared to the static Poisson's ratio throughout the section. The trends in dynamic and static Poisson's ratio with section height are different. The values of the static Poisson's ratio increase from 0.24 to approximately 0.30 in the vicinity of the Whale Stones. Above the Whale Stones, the values decrease again from approximately 0.40 to 0.28 towards the top of the Jet Rock Member. The dynamic and static Young's modulus and Poisson's ratio vary for different samples taken from the same sample block. This shows that there is a variation in elastic properties on centimetre scale laterally and meter scale vertically. The uniaxial compressive strength (UCS) ranges between 58 and 75 MPa (Fig. 5c).

The elastic properties are plotted against the amount of clay content for each Whitby shale sample (Fig. 6). This study shows that there is a moderate correlation between the clay content and the static Young's modulus ($R^2 \sim 0.5$) and a weak correlation between clay content and a dynamic Young's modulus ($R^2 \sim 0.3$) (Fig. 6a). The Young's modulus seems to decrease with an increase in clay content. There is no obvious correlation between the clay content and Poisson's ratio (Fig. 6b).

3.4. Brittleness of the WMF

Different rock characteristics, including mineral composition data, ultrasonic measurements and rock mechanics were used to predict the brittle deformation behaviour of the WMF throughout the stratigraphic section.

B_1 defines the brittleness as relative quartz content of the shale. The brittleness is low (0.07–0.25) throughout the stratigraphic section, due to the relatively high clay content of the WMF (40–75 wt%) (Fig. 7a). The most favourable conditions (varying from 0.54 up to 0.92) for brittle deformation are predicted by using the relation between elastic strain and total strain at failure (B_2) (Fig. 7b). Predicting the brittleness based on P- and S-wave data deduced from laboratory experiments (B_3) gives a wide variation in brittleness throughout the section. In the lower half of the section the brittleness index is about 0.5 and increases in the upper half to about 0.85 (Fig. 7c). B_4 is obtained from the normalised dynamic Young's Modulus and Poisson's ratio (Jin et al., 2014; Rickman et al., 2008) and based on the minimum and maximum Young's modulus and Poisson's ratio for the stratigraphic section. The brittleness index increases with an increasing dynamic Young's modulus (E) and decreasing dynamic Poisson's ratio (ν). An average brittleness index of about 0.50 with limited variation throughout the section is predicted (Fig. 7d).

Significant heterogeneity is observed in the brittle deformation behaviour throughout the stratigraphic section of the WMF, even though a single method was used to quantify the brittleness.

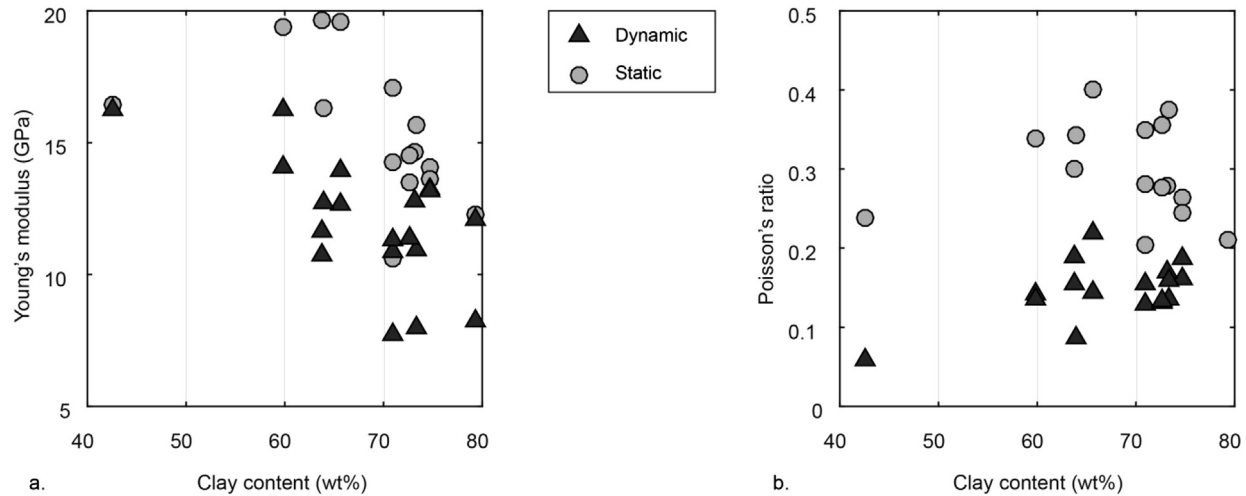


Fig. 6. Correlation between clay content and elastic properties of the Whitby Mudstone samples. a. Clay content versus Young's modulus. b. Clay content versus Poisson's ratio.

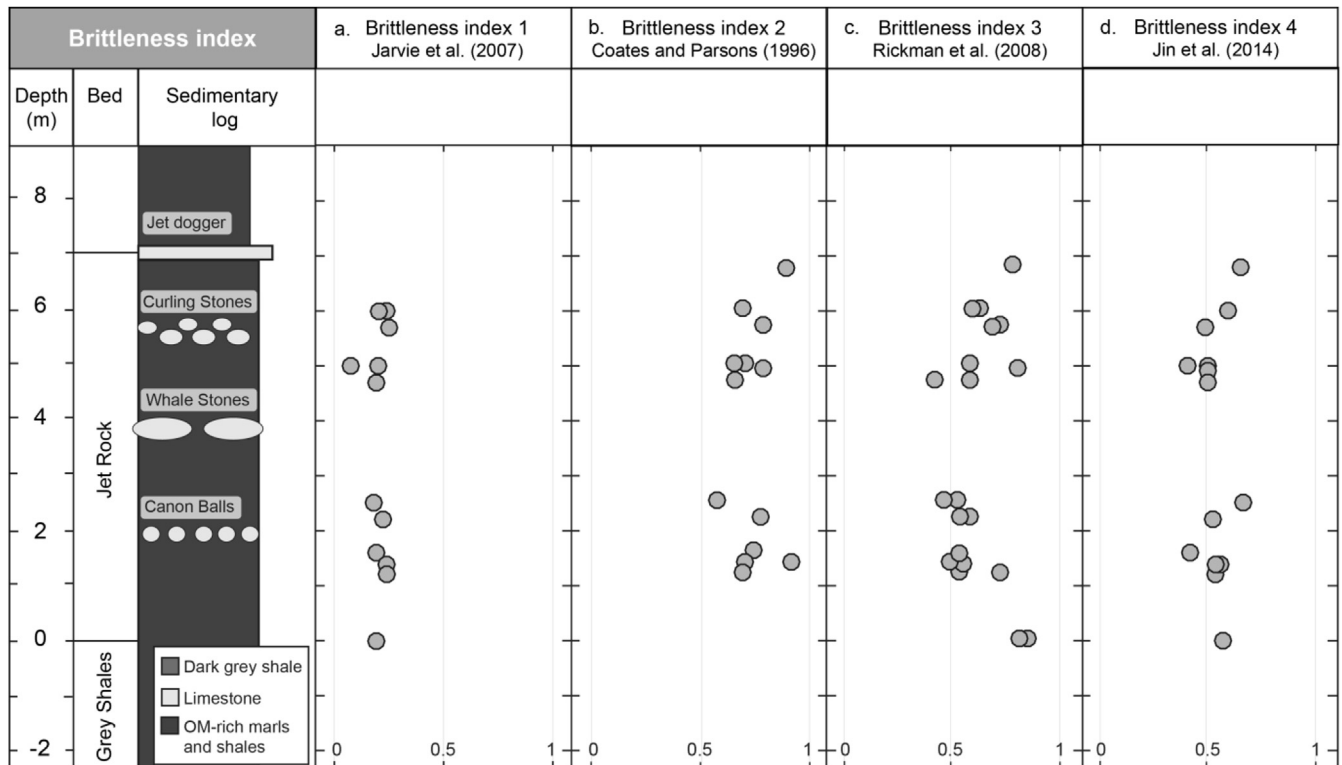


Fig. 7. Predictions of the brittle deformation behaviour of the WMF throughout the stratigraphic section calculated a. from the relative quartz content (B_1) (Jarvie et al., 2007), b. relation between elastic strain and total strain at failure (B_2) (Coates and Parsons, 1996), c. relation between dynamic Young's modulus and Poisson's ratio (B_3) (Rickman et al., 2008), d. and the relation between the minimum and maximum Young's modulus and Poisson's ratio (B_4) (Jin et al., 2014).

Additionally, the different methods used to quantify the brittleness show different values, because each brittleness index is based on different rock characteristics. The method used to quantify the brittleness influences therefore the prediction of the brittle deformation behaviour of the WMF. This discrepancy calls for a better prediction of the brittle deformation behaviour as is also stimulated by e.g., Holt et al. (2015) and Rybacki et al. (2016).

4. Comparison with other shales

4.1. Mineralogy and petrophysics comparison

The mineralogical composition of the WMF is compared to other Posidonia shales (Chesapeake, 2010; Gasparik et al., 2014; Ghanizadeh et al., 2014; Houben et al., 2016a,b;

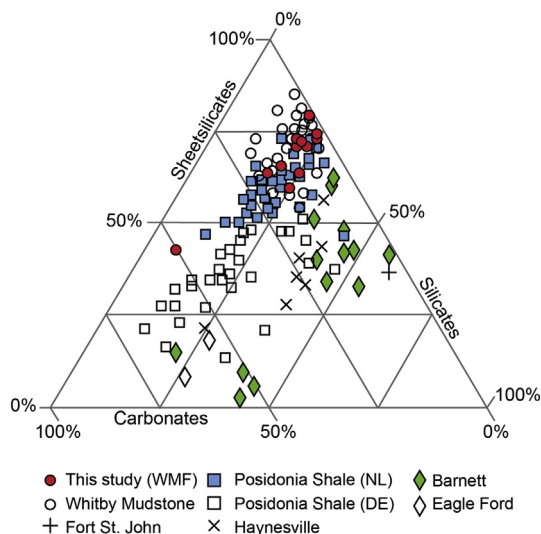


Fig. 8. Mineralogy of the WMF compared to other Posidonia Shales (Chesapeake, 2010; Gasparik et al., 2014; Ghanizadeh et al., 2014; Houben et al., 2016a, b; Kanitpanyacharoen et al., 2012; Klaver et al., 2015, 2012; Mathia et al., 2016; Rexer et al., 2014; Rybacki et al., 2016) and prospective US shales (Gasparik et al., 2014; Klaver et al., 2015; Sone and Zoback, 2013).

Kanitpanyacharoen et al., 2012; Klaver et al., 2016, 2015, 2012; Mathia et al., 2016; Rexer et al., 2014; Rybacki et al., 2016) and prospective US shales, including the Barnett, Haynesville, Eagle Ford, and Fort St. John (Gasparik et al., 2014; Klaver et al., 2015; Sone and Zoback, 2013) (Fig. 8). Both the Posidonia Shale in the Netherlands and the WMF are relatively rich in sheet silicates. The Posidonia Shale from Germany, however, shows a higher carbonate content and a lower sheet silicate content compared to the WMF, whereas the silicate content is similar (e.g., Houben et al., 2016b). The prospective US gas shales have in common that they are relatively low in sheet silicate minerals (<60%) and show a large scatter in the carbonate and silicate content (Fig. 8) (Houben et al., 2016a). This suggests that there is significant variation in mineral composition between shales from different basins.

4.2. Velocity and anisotropy comparison

Sone and Zoback (2013) observed a positive correlation between the clay and kerogen content and the elastic anisotropy of US shales from different basins (Fig. 9). However, this study does not adhere to the general trend of Sone and Zoback (2013). The P-wave and S-wave anisotropy is lower for the Whitby Mudstone than expected from Sone and Zoback (2013). The variation in properties within one set of samples taken from the same depositional basin (Whitby Mudstone), does not show any correlation between clay content and elastic anisotropy.

Trends in the degree of elastic anisotropy as a function of vertical velocities in US shales from different basins were reported by e.g., Sone and Zoback (2013) and Tsuneyama and Mavko (2005) (Fig. 10). However, this study does not show a correlation between the degree of elastic anisotropy and vertical velocities. This is consistent with the observations of Vernik and Liu (1997) on shales from different basins with a wide range of lithologies and maturity levels. An increase in P-wave anisotropy with increasing S-wave anisotropy is observed in this study, which is consistent with previous studies (e.g., Sone and Zoback, 2013; Vernik and Liu, 1997) (Fig. 10c).

4.3. Elastic properties comparison

The results of this study show a weak negative correlation between the clay content and Young's modulus on the outcrop scale (Fig. 6a). When comparing these parameters with samples of US shales from different basins (Sone and Zoback, 2013), the Young's modulus values obtained in this study are relatively low (~10–20 GPa) and the clay content is high (~60–80%). These values may fit the trend of decreasing Young's modulus with increasing clay and kerogen content as shown by Sone and Zoback (2013) (Fig. 11a), even though the experiments performed on dry shale samples by Sone and Zoback (2013) were conducted under confined pressure conditions. Confining pressure will influence the elastic behaviour of shales (e.g., Josh et al., 2012; Rybacki et al., 2015). Overall, the studies (e.g., Rybacki et al., 2015; Sone and Zoback, 2013) show a relatively low Young's modulus for a high clay content material, such as the Posidonia shales in Northwest

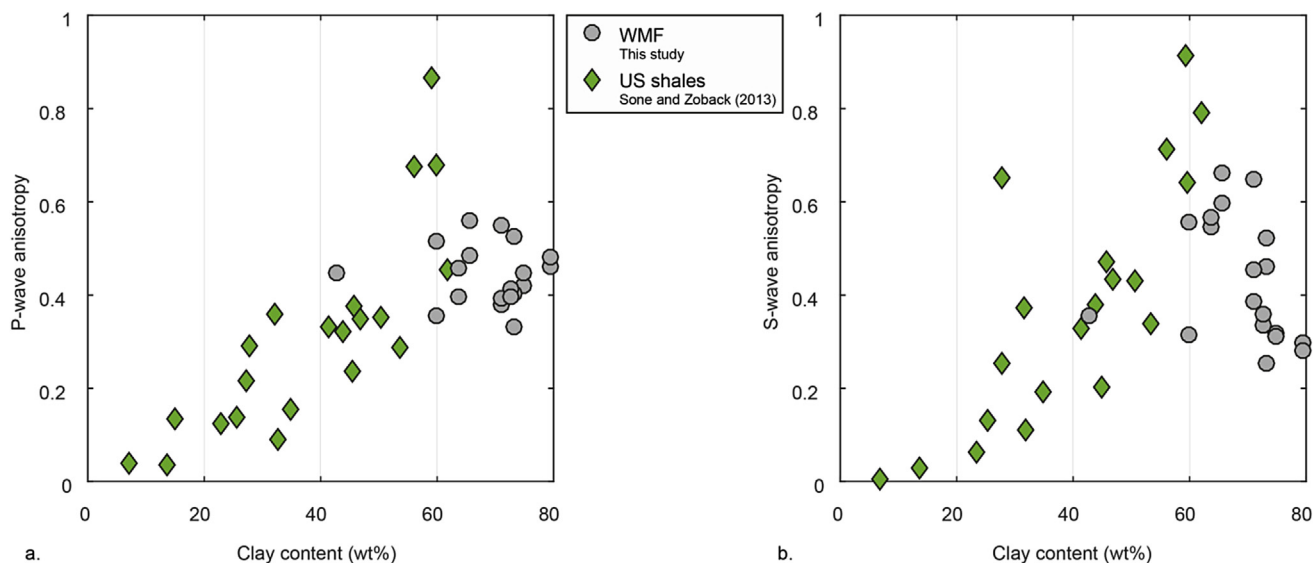


Fig. 9. Correlation between clay content and P-wave and S-wave anisotropy for the WMF compared to US shales from different basins (Sone and Zoback, 2013). a. Clay content versus P-wave anisotropy (ϵ). b. Clay content versus S-wave anisotropy (γ).

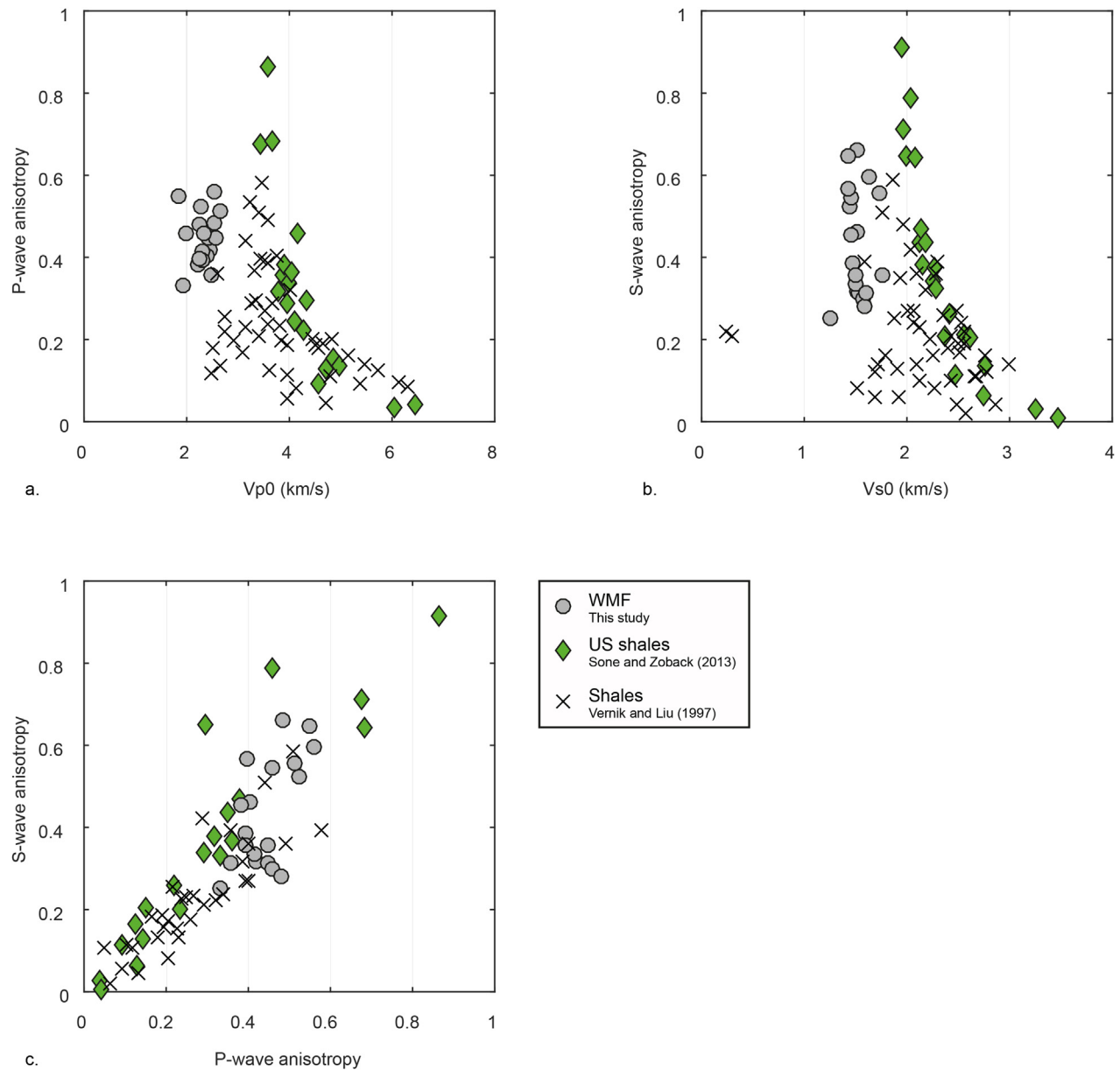


Fig. 10. Correlation between a. horizontal P-wave velocity and P-wave anisotropy (ϵ), b. horizontal S-wave velocity and S-wave anisotropy (γ), c. P-wave anisotropy (ϵ) and S-wave anisotropy (γ) of the WMF compared with shales from different basins (Sone and Zoback, 2013; Vernik and Liu, 1997).

Europe. No correlation was observed between shale composition and Poisson's ratio which is consistent with previous studies (e.g., Sone and Zoback, 2013) (Fig. 11b).

4.4. Brittleness comparison

Predictions of the brittle deformation behaviour of the WMF were based on different rock characteristics (mineralogy, elastic parameters, and the relation between elastic strain and total strain at failure), therefore showing significant variations throughout the stratigraphic section and between the different methods used to quantify the brittle deformation behaviour.

The brittle deformation behaviour of the WMF is compared to prospective gas shales including the Barnett, Haynesville, Eagle Ford and Forth St. John shales (Gasparik et al., 2014; Klaver et al., 2015; Rybacki et al., 2016; Sone and Zoback, 2013). When comparing the brittleness index calculated as a function of relative

quartz content (B_1) of the WMF to prospective US shales, the brittleness of the WMF is relatively low (Fig. 12). The low brittleness value is due to the relatively low quartz content in the WMF. This suggests that the WMF is less prone to mechanically fracturing compared to producing US shales. Comparing the brittleness, based on rock mechanical data (B_2 , B_3 , and B_4) of the WMF, to producing US shales is complicated. The experimental conditions used in this study and previous studies (e.g., confining pressure, temperature, water saturation) on brittle deformation behaviour differ from each other (e.g., Holt et al., 2015, 2011; Jarvie et al., 2007; Rickman et al., 2008; Rybacki et al., 2016; Yang et al., 2013). Since confining pressure and temperature influence the rock mechanical properties and, hence, the brittle behaviour of a shale (Josh et al., 2012; Rybacki et al., 2015; Yang et al., 2013), no comparison of brittleness was made based on the ultrasonic measurements and rock mechanical data.

Different methods of determining the brittleness index for the

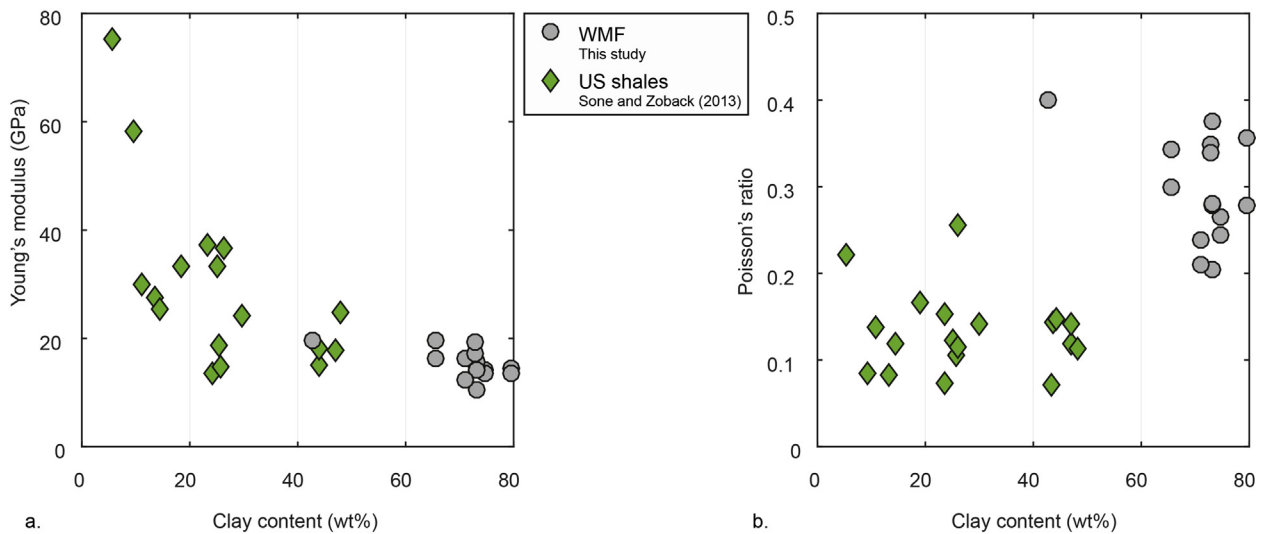


Fig. 11. Correlation between clay content and a. Young's modulus, b. Poisson's ratio of the WMF compared to US shales from different basins (Sone and Zoback, 2013).

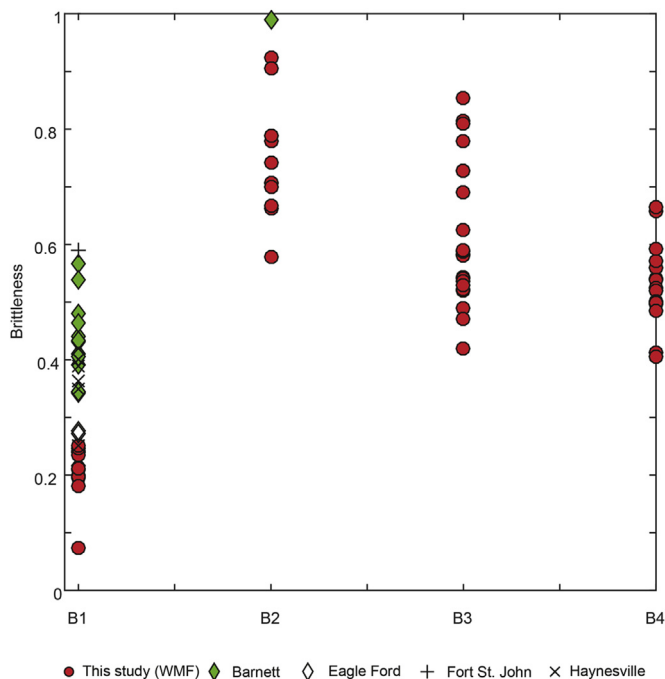


Fig. 12. Brittleness indices based on different rock characteristics of the WMF compared with US shales from different basins (Gasparik et al., 2014; Klaver et al., 2015; Rybacki et al., 2016; Sone and Zoback, 2013).

same sample results in a significant variation in brittle deformation behaviour. Based on B_1 the WMF is expected to behave ductile, whereas based on B_2 the WMF is expected to behave more brittle. B_3 and B_4 predict a mixed brittle/ductile behaviour for the WMF. A more uniform method of determining the brittleness index is necessary so that predictions do not depend on the used method.

5. Validity of generic trends

5.1. Heterogeneity scale

Shale gas reservoirs consist of multiple depositional units, which create significant variation in lithology, petrophysical

properties, elastic anisotropy, and rock-mechanical behaviour (e.g., Passey et al., 2010; Sone and Zoback, 2013). This heterogeneity may influence the fluid-flow pathways, brittleness, stress concentration around the wellbore, fracture response, and ultimately oil or gas recovery efficiency. Furthermore, it may complicate the predictions of deformation behaviour of shales (Ambrose et al., 2008; Maxwell et al., 2011; Suarez-Rivera et al., 2006).

Houben et al. (2016a, b) observed significant variation in mineralogical and petrophysical properties in the Whitby Mudstone samples on the millimetre scale based on Scanning Electron Microscope (SEM) mosaics. Porosity varies with measuring method (Busch et al., 2016; Houben et al., 2014, 2016a) due to the fact that different methods measure porosity at different resolutions and the lateral and vertical variation naturally present in the rock (Houben et al., 2016a). The WMF samples show that the highest percentage of pores are present in the clay matrix as intergranular pores where highest matrix porosity coincides with a low overall matrix content (Houben et al., 2016a). All analyses in this study were performed on centimetre-scale Whitby Mudstone samples. All centimetre-scale samples were anisotropic and show preferred bedding orientation and mineralogically different layers. The samples were early mature and organic matter is oriented mainly parallel to the bedding (Houben et al., 2016a,b). The cylinder-shaped samples did not show any damage (e.g., large pores or fractures) from the samples outside before deformation. This implies that the undamaged microstructures visualised by Houben et al. (2016a, b) could be applied here. At the cm-scale, microstructures consist of minerals floating within a fine-grained clay matrix with the presence of some cracks (Houben et al., 2016a, b).

This study shows that significant heterogeneity in mineralogy, petrophysical properties, elastic anisotropy, and rock-mechanical behaviour is observed on an outcrop scale. A significant heterogeneity is also present in the US shales reported by Sone and Zoback (2013) within a narrow range in clay content (e.g. Fig. 9a; clay content 20–40 wt%; P-wave anisotropy between ~0.1 and ~0.4). The heterogeneity in shale mineralogy and petrophysical properties may be caused by depositional fluctuations. When comparing the heterogeneities in mineralogy and petrophysical properties on an outcrop scale with shales from different basins, the heterogeneity on an outcrop scale is more confined, but is still significant. The presence of significant heterogeneities in rock properties on

various scales, and the different methods used to quantify the brittle deformation of shales complicates predictions on brittle deformation behaviour and hence the fracture initiation and propagation throughout a reservoir.

5.2. Fit to trends

Finding generic trends in mechanical and physical rock properties is important to be able to make predictions on, e.g., the fracture response, which is crucial for successful production from shale reservoirs.

This study shows no obvious correlation within the Whitby Mudstone between: (1) clay content and elastic anisotropy, (2) vertical velocity and elastic anisotropy, and (3) clay content and elastic parameters. Only a weak to moderate correlation between the clay content and Young's modulus is present on an outcrop scale (Fig. 6a). The weak correlation observed on an outcrop scale implies that not only clay content controls the stiffness of the shales. A simple generic trend in mechanical and physical properties does not exist on an outcrop scale within the Whitby Mudstone due to the complexity of shales. When comparing US shales from different basins, however, a correlation between the clay content and Young's modulus is present (Fig. 11). An overall decrease in Young's modulus with increasing clay content reflects a larger amount of compliant materials (clay and organics) and a smaller amount of stiff minerals (quartz and carbonates) (Sone and Zoback, 2013).

Sone and Zoback (2013) compared US shales from different basins and observed an increase in elastic anisotropy with increasing clay and kerogen content. This correlation may be the result of the anisotropic behaviour of the clay minerals itself and the anisotropic fabric created by the preferred orientation of clay minerals (Johnston and Christensen, 1996; Sone and Zoback, 2013). Sone and Zoback (2013) suggested that the high degree of anisotropy is also related to the high maturity exhibited in the shale samples, influencing the kerogen distribution and microcrack alignment (Vanorio et al., 2008). However, the study of Sone and Zoback (2013) also observed a low degree of anisotropy (i.e., <0.2) in some samples even though all the analysed samples are mature (Fig. 9). This implies that also other parameters than maturity causes the trend as observed by Sone and Zoback (2013). Additionally, Sone and Zoback (2013) suggested that the observed confined trends between the degree of anisotropy and vertical velocities may be caused by the narrow range in maturity exhibited in the US shales from different basins. Microfabric observations showed that the kerogen is oriented parallel to the bedding in mature shales, whereas the kerogen becomes finely scattered in postmature shales (Sone and Zoback, 2013). However, this trend was not observed in this study, even though all the analysed Whitby shale samples were early mature and the organic matter is oriented mainly parallel to the bedding (Houben et al., 2016a). The absence of a correlation between vertical velocities and elastic anisotropy is consistent with the observations of Vernik and Liu (1997), who analysed organic-rich samples of shales from different basins that exhibit a wide range of maturation levels (i.e., immature to post-mature).

The results suggest that there is no single parameter that influences the elastic anisotropy and, hence, the correlation between the vertical velocity and elastic anisotropy in shales, such as maturity or clay and kerogen content. Sondergeld and Rai (2011) suggest that there are multiple causes of anisotropy in shales, including alignment of clay platelets, organic matter, stresses, and fractures. Hornby (1998) suggested that compaction resulted in increased clay particle alignment which causes an increase in anisotropy. The presence of bedding planes (Vernik and Nur, 1992;

Zhubayev et al., 2016) and microcracks oriented parallel to the bedding (Vernik and Nur, 1992) enhance the anisotropy. Houben et al. (2014) and Sayers (2008) suggest that the shape and orientation of the pore space influences the anisotropy and may be different for clay-rich and quartz-rich shales. Pores are mainly oriented parallel to the bedding in clay-rich shales (Houben et al., 2016a, b), whereas pores are more randomly orientated when the amount of quartz increases (Houben et al., 2014). The wide range of causes for shale anisotropy complicate the interpretation of anisotropy calculations and, hence, correlations made on shales on an outcrop scale.

A generic trend is present when the average of the samples from a single formation based on composition is taken and this trend for WMF fit to the trends of shales from different basins of Sone and Zoback (2013). However, this trend is not visible on an outcrop scale. This study shows that on an outcrop scale variation in one parameter cannot automatically be translated to variation in another parameter. Parameters other than mineralogy also contribute to the behaviour of these complex shales; these parameters include the above mentioned alignment of clay platelets, presence of bedding, organic matter, stresses, and fractures. This complexity of shales may cause significant spread in the parameters at a narrow range in clay content, and thus the absence of clear correlations. Further examination on microstructures and pore characteristics in shales is required to understand which parameters cause the absence of trends on an outcrop scale.

The presence of a trend when comparing shales from different basins may be caused by the large variation in properties. The variation in clay content for the WMF is lower (60–80%) than that of shale samples from different basins. Shales with a relative low clay content (e.g. ~20%) will always have a lower anisotropy or Young's modulus than shales with a very high clay content (e.g. ~80%). The influence of parameters other than mineralogy might become less prominent when comparing shales from different basins. The trends observed by Sone and Zoback (2013) can thus be used when comparing different basins, but they are not necessarily applicable to outcrop scale or well log scales.

6. Conclusions

A significant variability in mineralogical, petrophysical, anisotropy, and rock-mechanical properties were found on an outcrop scale in the Whitby Mudstone. Heterogeneity in mineral composition is more confined when the Whitby Mudstone is compared to shales consisting of a wide range of lithologies and from different basins. There are no obvious correlations between mineral composition and elastic properties in the Whitby Mudstone (outcrop scale), whereas the elastic properties seem to be a function of composition when a wider range of lithologies from different basins is included in the analysis. The anisotropy, described by Thomsen parameters, does not correlate with mineral content on an outcrop scale. No correlation between anisotropy and vertical velocities is found for the Whitby Mudstone, which is inconsistent with previous studies on shales from different basins. The generic trends used to describe the anisotropy and rock-mechanical properties defined by other studies, cannot always be applied to all types of gas shales at any scale. Multiple parameters will contribute to the behaviour of shales. The complexity in shales makes it difficult to find generic trends on an outcrop scale. Comparison with shales from different basins show, however, generic trends in rock-mechanical and rock-physical properties. The significant higher variation in lithology, hence rock-mechanical properties, between shales from different basins causes that the influence of parameters other than mineralogy become less prominent on a basin scale.

Acknowledgements

Funding from the Dutch Upstream Gas top-sector initiative (project no. TKIG01020) and our industry partners EBN B.V., Engie E&P NL B.V., Wintershall Noordzee B.V., and Baker Hughes NL B.V. is acknowledged. The constructive reviews by two anonymous reviewers are greatly appreciated.

References

- Ambrose, W.A., Lakshminarasimhan, S., Holtz, M.H., Nunez-Lopez, V., Hovorka, S.D., Duncan, I., 2008. Geologic factors controlling CO₂ storage capacity and permanence: case studies based on experience with heterogeneity in oil and gas reservoirs applied to CO₂ storage. *Environ. Geol.* 54, 1619–1633. <http://dx.doi.org/10.1007/s00254-007-0940-2>.
- Britt, L.K., Schoeffler, J., 2009. The geomechanics of a shale Play: what makes a shale prospective. In: SPE Eastern Regional Meeting. Society of Petroleum Engineers. <http://dx.doi.org/10.2118/125525-MS>.
- Busch, A., Schweinar, K., Kampman, N., Coorn, A., Pipich, V., Feoktystov, A., Bertier, P., 2016. Shale Porosity-What Can We Learn from Different Methods? In Fifth EAGE Shale Workshop. <http://dx.doi.org/10.3997/2214-4609.201600391>.
- Chesapeake, 2010. Posidonia Cutting Researchm 26th of July 2010 available through. www.nlog.nl.
- Coates, D.F., Parsons, R.C., 1966. Experimental criteria for classification of rock substances. *Int. J. Rock Mech. Min. Sci.* 3, 181–189. [http://dx.doi.org/10.1016/0148-9062\(66\)90022-2](http://dx.doi.org/10.1016/0148-9062(66)90022-2).
- Dewhurst, D.N., Siggins, A.F., 2006. Impact of fabric, microcracks and stress field on shale anisotropy. *Geophys. J. Int.* 165, 135–148. <http://dx.doi.org/10.1111/j.1365-246X.2006.02834.x>.
- Ewy, R., Bovberg, C., Stankovic, R., 2010. Strength Anisotropy of Mudstones and Shales, 44th US Rock Mech. Symp. 5th US-Canada Rock Mech. Symp. <http://dx.doi.org/10.1017/CBO9781107415324.004>.
- Fjær, E., Nes, O.M., 2014. The impact of heterogeneity on the anisotropic strength of an outcrop shale. *Rock Mech. Rock Eng.* 47, 1603–1611. <http://dx.doi.org/10.1007/s00603-014-0598-5>.
- Frimmel, A., Oschmann, W., Schwark, L., 2004. Chemostratigraphy of the Posidonia Black Shale, SW Germany I. Influence of sea-level variation on organic facies evolution. *Chem. Geol.* 206, 199–230. <http://dx.doi.org/10.1016/j.chemgeo.2003.12.007>.
- Gasparik, M., Bertier, P., Gensterblum, Y., Ghanizadeh, A., Krooss, B.M., Littke, R., 2014. Geological controls on the methane storage capacity in organic-rich shales. *Int. J. Coal Geol.* 123, 34–51. <http://dx.doi.org/10.1016/j.coal.2013.06.010>.
- Ghanizadeh, A., Amann-Hildenbrand, A., Gasparik, M., Gensterblum, Y., Krooss, B.M., Littke, R., 2014. Experimental study of fluid transport processes in the matrix system of the European organic-rich shales: II. Posidonia Shale (Lower Toarcian, Northern Germany). *Int. J. Coal Geol.* 123, 20–33. <http://dx.doi.org/10.1016/j.coal.2013.06.009>.
- Herber, R., Jager, J. De, 2010. Geoprospective oil and gas in The Netherlands – is there a future? *Neth. J. Geosci.* 89, 91–107. <http://dx.doi.org/10.1017/S001677460000072X>.
- Hesselbo, S.P., Grocke, D.R., Jenkens, H.C., Bjerrum, C.J., Farrimond, P., Bell, H.S.M., Green, O.R., 2000. Massive dissociation of gas hydrate during a Jurassic oceanic anoxic event. *Nature* 406, 392–395. <http://dx.doi.org/10.1038/35019044>.
- Holt, R.M., Fjær, E., Nes, O.M., Allassi, H.T., 2011. A Shaly Look at Brittleness, 45th US Rock Mech. Geomech. Symp., pp. 1–10.
- Holt, R.M., Fjær, E., Stenebråten, J.F., Nes, O.-M., 2015. Brittleness of shales: relevance to borehole collapse and hydraulic fracturing. *J. Pet. Sci. Eng.* 131, 200–209. <http://dx.doi.org/10.1016/j.petrol.2015.04.006>.
- Hornby, B.E., 1998. Experimental laboratory determination of the dynamic elastic properties of wet, drained shales. *J. Geo. Res.* 103, 29945–29964. <http://dx.doi.org/10.1029/97JB02380>.
- Houben, M.E., Barnhoorn, A., Lie-A-Fat, J., Ravestein, T., Peach, C.J., Drury, M.R., 2016a. Microstructural characteristics of the Whitby Mudstone Formation (UK). *Mar. Pet. Geol.* 70, 185–200. <http://dx.doi.org/10.1016/j.marpetgeo.2015.11.011>.
- Houben, M.E., Barnhoorn, A., Wasch, L., Trabucho-Alexandre, J., Peach, C.J., Drury, M.R., 2016b. Microstructures of early Jurassic (toarcian) shales of Northern Europe. *Int. J. Coal Geol.* 165, 76–89. <http://dx.doi.org/10.1016/j.coal.2016.08.003>.
- Houben, M.E., Desbois, G., Urai, J.L., 2014. A comparative study of representative 2D microstructures in Shaly and Sandy facies of Opalinus Clay (Mont Terri, Switzerland) inferred from BIB-SEM and MIP methods. *Mar. Pet. Geol.* 49, 143–161. <http://dx.doi.org/10.1016/j.marpetgeo.2013.10.009>.
- Hucka, V., Das, B., 1974. Brittleness determination of rocks by different methods. *Int. J. Rock Mech. Min. Sci.* 11, 389–392. [http://dx.doi.org/10.1016/0148-9062\(74\)91109-7](http://dx.doi.org/10.1016/0148-9062(74)91109-7).
- Jarvie, D.M., Hill, R.J., Ruble, T.E., Pollastro, R.M., 2007. Unconventional shale-gas systems: the Mississippian Barnett Shale of north-central Texas as one model for thermogenic shale-gas assessment. *Am. Assoc. Pet. Geol. Bull.* 91, 475–499. <http://dx.doi.org/10.1306/12190606068>.
- Jenkens, B.H.C., 1985. The Early Toarcian and Cenomanian-Turonian anoxic events in Europe: comparisons and contrasts. *Geol. Rundsch.* 74, 505–518. <http://dx.doi.org/10.1007/BF01821208>.
- Jun, X., Shah, S.N., Roegiers, J.-C., Zhang, B., 2014. Fracability evaluation in shale reservoirs—an integrated petrophysics and geomechanics approach. In: SPE Hydraulic Fracturing Technology Conference. Society of Petroleum Engineers, pp. 1–14. <http://dx.doi.org/10.2118/168589-MS>.
- Johnston, J.E., Christensen, N.I., 1996. Seismic anisotropy of shales. *Int. J. Rock Mech. Min. Sci. Geomech. Abstr.* 33, 72A. <http://dx.doi.org/10.1029/95JB00031>, 72A(1).
- Josh, M., Esteban, L., Plane, C.D., Sarout, J., Dewhurst, D.N., Clennell, M.B., 2012. Laboratory characterisation of shale properties. *J. Pet. Sci. Eng.* 88–89, 107–124. <http://dx.doi.org/10.1016/j.petrol.2012.01.023>.
- Kanitpanyacharoen, W., Kets, F.B., Wenk, H.R., Wirth, R., 2012. Mineral preferred orientation and microstructure in the Posidonia Shale in relation to different degrees of thermal maturity. *Clays Clay Min.* 60, 315–329. <http://dx.doi.org/10.1346/CCMN.2012.0600308>.
- Klaver, J., Desbois, G., Littke, R., Urai, J.L., 2016. BIB-SEM pore characterization of mature and post mature Posidonia Shale samples from the Hills area, Germany. *Int. J. Coal Geol.* 158, 78–89. <http://dx.doi.org/10.1016/j.coal.2016.03.003>.
- Klaver, J., Desbois, G., Littke, R., Urai, J.L., 2015. BIB-SEM characterization of pore space morphology and distribution in postmature to overmature samples from the Haynesville and Bossier Shales. *Mar. Pet. Geol.* 59, 451–466. <http://dx.doi.org/10.1016/j.marpetgeo.2014.09.020>.
- Klaver, J., Desbois, G., Urai, J.L., Littke, R., 2012. BIB-SEM study of the pore space morphology in early mature Posidonia Shale from the hills area, Germany. *Int. J. Coal Geol.* 103, 12–25. <http://dx.doi.org/10.1016/j.coal.2012.06.012>.
- Littke, R., Leythaeuser, D., Rullkötter, J., Baker, D.R., 1991. Keys to the depositional history of the Posidonia Shale (Toarcian) in the Hills Syncline, northern Germany. *Geol. Soc. Lond. Spec. Publ.* 58 (1), 311–333. <http://dx.doi.org/10.1016/j.marpetgeo.2015.11.011>.
- Mathia, E.J., Bowen, L., Thomas, K.M., Aplin, A.C., 2016. Evolution of porosity and pore types in organic-rich, calcareous, lower Toarcian Posidonia shale. *Mar. Pet. Geol.* 75, 117–139. <http://dx.doi.org/10.1016/j.marpetgeo.2016.04.009>.
- Mavko, G., Mukerji, T., Dvorkin, J., 2003. *The Rock Physics Handbook: Tools for Seismic Analysis of Porous Media*. Cambridge university press, pp. 17–50.
- Maxwell, S.C., Cho, D., Pope, T., Jones, M., Cipolla, C., Mack, M., Norton, F.H.S.M., Energy, J.L.P., 2011. Enhanced reservoir characterization using hydraulic fracture microseismicity. In: SPE Hydraulic Fracturing Technology Conference. Society of Petroleum Engineers. <http://dx.doi.org/10.2118/140449-MS>.
- Passey, Q.R., Bohacs, K.M., Esch, W.L., Klimentidis, R., Sinha, S., Upstream, E., 2010. From oil-prone source rock to gas-producing shale reservoir – geologic and petrophysical characterization of unconventional shale-gas reservoirs. In: International Oil & Gas Conference and Exhibition in China. Society of Petroleum Engineers, pp. 1707–1735. <http://dx.doi.org/10.2118/131350-MS>.
- Powell, J.H., 2010. Jurassic sedimentation in the Cleveland basin: a review. *Proc. Yorksh. Geol. Soc.* 58, 21–72. <http://dx.doi.org/10.1144/pygs.58.1.278>.
- Rexer, T.F., Mathia, E.J., Aplin, A.C., Thomas, K.M., 2014. High-pressure methane adsorption and characterization of pores in posidonia shales and isolated kerogens. *Energy Fuels* 28, 2886–2901. <http://dx.doi.org/10.1021/ef402466m>.
- Rickman, R., Mullen, M., Petre, E., Grieser, B., Kundert, D., 2008. A practical use of shale petrophysics for stimulation design optimization: all shale plays are not clones of the Barnett Shale. In: SPE Annual Technical Conference and Exhibition. Society of Petroleum Engineers, pp. 1–11. <http://dx.doi.org/10.2118/115258-MS>.
- Rybacki, E., Meier, T., Dresen, G., 2016. What controls the mechanical properties of shale rocks? - part II Brittleness. *J. Pet. Sci. Eng.* 144, 39–58. <http://dx.doi.org/10.1016/j.petrol.2016.02.022>.
- Rybacki, E., Reinicke, A., Meier, T., Makasi, M., Dresen, G., 2015. What controls the mechanical properties of shale rocks? - Part I: strength and Young's modulus. *J. Pet. Sci. Eng.* 135, 702–722. <http://dx.doi.org/10.1016/j.petrol.2016.02.022>.
- Sayers, C.M., 2008. The effect of low aspect ratio pores on the seismic anisotropy of shales. In: 2008 SEG Annual Meeting. Society of Exploration Geophysicists, pp. 2750–2754. <http://dx.doi.org/10.1190/1.3063916>.
- Sondergeld, C., Rai, C., 2011. Elastic anisotropy of shales. *Lead. Edge* 30 (3), 324–331.
- Sone, H., Zoback, M.D., 2013. Mechanical properties of shale-gas reservoir rocks - Part 1: static and dynamic elastic properties and anisotropy. *Geophysics* 78, D381–D392. <http://dx.doi.org/10.1190/geo2013-0050.1>.
- Suarez-Rivera, R., Green, S., McLennan, J., Bai, M., 2006. Effect of layered heterogeneity on fracture initiation in tight gas shales. In: SPE Annual Technical Conference and Exhibition. Society of Petroleum Engineers. <http://dx.doi.org/10.2118/103327-MS>.
- Ter Heege, J., Zijp, M., Nelskamp, S., Douma, L., Verreussel, R., Ten Veen, J., Peters, R., 2015. Sweet spot identification in underexplored shales using multidisciplinary reservoir characterization and key performance indicators: example of the Posidonia Shale formation in The Netherlands. *J. Nat. Gas. Sci. Eng.* 27, 558–577. <http://dx.doi.org/10.1016/j.jngse.2015.08.032>.
- Thomsen, L., 1986. Weak elastic anisotropy. *Geophysics* 51 (10), 1954–1966. <http://dx.doi.org/10.1190/1.1442051>.
- Tsuneyama, F., Mavko, G., 2005. Velocity anisotropy estimation for brine-saturated sandstone and shale. *Lead. Edge* 24 (9), 882–888. <http://dx.doi.org/10.1190/1.2056371>.
- Van Bergen, F., Zijp, M.H.A.A., Nelskamp, S., Kombrink, H., 2013. Shale gas evaluation of the early Jurassic posidonia shale formation and the carboniferous epen formation in The Netherlands. *AAPG Hedb. Mem.* 103, 1–24. <http://dx.doi.org/10.1306/13401722H53468>.
- Vanorio, T., Mukerji, T., Mavko, G., 2008. Emerging methodologies to characterize the rock physics properties of organic-rich shales. *Lead. Edge* 27 (6), 780–787. <http://dx.doi.org/10.1190/1.2944165>.
- Vernik, L., Liu, X., 1997. Velocity anisotropy in shales: a petrophysical study.

- Geophysics 62 (2), 521–532. <http://dx.doi.org/10.1190/1.1444162>.
- Vernik, L., Nur, A., 1992. Ultrasonic velocity and anisotropy of hydrocarbon source rocks. *Geophysics* 57 (5), 727–735. <http://dx.doi.org/10.1190/1.1443286>.
- Warpinski, N.R., Teufel, L.W., 1987. Influence of geologic discontinuities on hydraulic fracture propagation (includes associated papers 17011 and 17074). *J. Pet. Tech.* 39 (02), 209–220. <http://dx.doi.org/10.2118/13224-PA>.
- Yang, Y., Sone, H., Hows, A., Zoback, M.D., 2013. Comparison of brittleness indices in organic-rich shale formations. In: 47th US Rock Mechanics/Geomechanics Symposium. American Rock Mechanics Association, pp. 1398–1404.
- Zhubayev, A., Houben, M.E., Smeulders, D.M.J., Barnhoorn, A., 2016. Ultrasonic velocity and attenuation anisotropy of shales, Whitby, United Kingdom. *Geophysics* 81 (1), D45–D56. <http://dx.doi.org/10.1190/geo2015-0211.1>.
- Zijp, M., Ten Veen, J., Verreussel, R., Heege, J. Ter, Ventra, D., Martin, J., 2015. Shale gas formation research: from well logs to outcrop - and back again. *First Break* 33 (2), 99–106.